Load Frequency Control in a Restructured Power System with Hydrogen Energy Storage unit with the Computation of Ancillary Service Requirement Assessment Indices

ND. Sridhar [1], I.A.Chidambaram [2]

Abstract— Power System Load Frequency Control (LFC) problems are caused even by the small load perturbations which continuously disturb the normal operation of the power system. The objectives of LFC are to minimize the transient deviations in area frequency and tie-line power interchange and to ensure their steady state error to be zero. This paper proposes the computation procedure for obtaining the Power System Ancillary Service Requirement Assessment Indices (PSASRAI) of a Two-Area Thermal Reheat Interconnected Power System (TATRIPS) in a restructured environment. These Indices indicates the Ancillary Service requirement to improve the efficiency of the physical operation of the power system. As Proportional plus Integral (PI) type controllers have wide usages in efficiently controlling the LFC problems. In this paper the PI controllers are adopted for the restructured power system and gain of the controllers are obtained using Bacterial Foraging Optimization (BFO) algorithm. These controllers are implemented to achieve a faster restoration time in the output responses of the system when the system experiences with various step load perturbations. These various PSASRAI are computed based on the settling time and peak over shoot of the control input deviations of each area. To ensure a faster settling time and reduced peak over shoot of the control input requirement, energy storage devices have an attractive option for meeting out the demands Here Hydrogen Energy Storage (HES) unit can be efficiently utilized to meet the peak demand and enhanced Power System Ancillary Service Requirement Assessment Indices. In this paper the PSASRAI are calculated for different types of transactions and the necessary remedial measures to be adopted are also suggested.

Index Terms— Ancillary Service, Bacterial Foraging Optimization, Hydrogen Energy Storage, Proportional plus Integral Controller, Power System Ancillary Service Requirement Assessment Indices, Restructured Power System.

I. INTRODUCTION

Power system composed of several interconnected control areas and the various areas are interconnected through tie-lines. The scheduled energy exchange between control areas is done by tie-lines. A small load fluctuation in any area causes the deviation of frequencies of all the areas and also in the tie-line power flow. These deviations have to be corrected through supplementary control. This supplementary control is basically referred as Load-Frequency Control (LFC). Maintaining frequency and power interchanges with interconnected control areas at the scheduled values are the major objectives of a LFC. The electric power business at present is largely in the hands of Vertically Integrated Utilities (VIU) which own generation, transmission and distribution systems that supply power to the customer at regulated rates. The electric power can be bought and sold between the interconnected VIU through the tie-lines and moreover such interconnection should provide greater reliability [1]. In an interconnected power system, a sudden load perturbation in any area causes the deviation of frequencies of all the areas and also in the tie-line powers. This has to be corrected to ensure the generation and distribution of electric power companies to ensure good quality [2]. This can be achieved by optimally tuning the Load-Frequency controller gains. Many investigations in the area of Load-Frequency Control (LFC) problem for the interconnected power systems in a deregulated environment have been reported over the past decades [3-7]. These studies try to modify the conventional LFC system to take into account the effect of bilateral contracts on the dynamics and improve the dynamic and transient response of the system under various operating conditions. The frequency and the interchanged power are kept at their desired values by means of feedback of the Area Control Error (ACE) integral, containing the frequency deviation and the error of the tie-line power, and controlling the prime movers of the generators. The controllers so designed regulate the ACE to zero [8, 9].

Ancillary services can be defined as a set of activities undertaken by generators, consumers and network service providers and coordinated by the system operator that have to maintain the availability and quality of supply at levels sufficient to validate the assumption of commodity like behavior in the main commercial markets. There are different types of ancillary services such as the real power generating capacity related voltage support, regulation, etc. In power generation capacity related Ancillary services are the one in which regulation is based on load following capability. Spinning Reserve (SR) based on Ancillary services is a type of operating reserve, which is a resource capacity synchronized to the system that is unloaded, is able to respond immediately to serve load, and is fully available within ten minutes. Non Spinning Reserve (NSR) based Ancillary services are the one in which NSR is not synchronized to the system and Replacement Reserve (RR) is a resource capacity non synchronized to the system, which is able to serve load normally within thirty or sixty minutes. Reserves can be

provided by generating units or interruptible load in some cases. Ancillary services can be divided into the following three categories and are listed below [10].   (i)

Frequency Control Ancillary Services (FCAS): This is related to spot market implementation, short-term energy-balance and power system frequency. (ii) Network Control Ancillary Services (NCAS): This is related to aspects of quality of supply other than frequency (primarily voltage magnitude and system security). (iii) System Restoration Ancillary Services (SRAS): This is related to system restoration or re-starts following major blackouts. Investigation of the power system markets shows that frequency control is one of the most profitable ancillary services. Load Frequency Control requirement should be expanded to include the planning functions necessary to insure the resources needed for LFC implementation. Thus, the LFC system keeps track of the momentary active power imbalance, detects it, corrects it and communicates an adequate amount of the balance energy services basis, to the market operating system [11].

In this paper various methodologies were adopted in computing Power System Ancillary Service Requirement Assessment Indices (PSASRAI) for Two-Area Thermal Reheat Interconnected Power System (TATRIPS) in a restructured environment. With the various Power System Ancillary Service Requirement Assessment Indices (PSASRAI) like Feasible Assessment Indices (FAI) or Feasible Ancillary Service Requirement Assessment Indices (FASRAI) Comprehensive Assessment Indices (CAI) or Comprehensive Ancillary Service Requirement Assessment Indices (CASRAI) the remedial measures to be taken can be adjudged like integration of additional spinning reserve, incorporation of effective intelligent controllers, load shedding etc. With the conventional frequency control, a governor may no longer be able to compensate for sudden load changes due to its slow response. Therefore, in an inter area mode, damping out the critical electromechanical oscillations is to be carried out effectively in the restructured power system. Moreover, the system's control input requirement should be monitored and remedial actions to overcome the control input deviation excursions are more likely to protect the system before it enters an emergency mode of operation. Special attention is therefore given to the behavior of network parameters, control equipments as they affect the voltage and frequency regulation during the restoration process which in turn reflects in PSASRAI.

Heuristic optimization techniques are general purpose methods that are very flexible and can be applied to many types of objectives functions and constraints [12]. Now-a-days the complexities in the power system are being solved with the use of Evolutionary Computation (EC) such as Bacterial Foraging Optimization [BFO] mimics how bacteria forage over a landscape of nutrients to perform parallel non-gradient optimization [13]. The BFO algorithm is a computational intelligence based technique that is not affected larger by the size and nonlinearity of the problem and can be convergence to the optimal solution in many problems where most analytical methods fail to converge. This more recent and powerful evolutionary computational technique BFO [14] is found to be user friendly and is adopted for simultaneous optimization of several parameters for both primary and secondary control loops of the governor. Most of the proposed LFC strategies have not been resulted as the most successful options due to system operational constraints associated with thermal power plants. The main reason is the non-availability of required power other than the stored energy in the generator rotors, which can improve the performance of the system, in the wake of sudden increased load demands. In order to compensate for sudden load changes, an active power source with fast response such as Hydrogen Energy Storage (HES) has a wide range of applications such as power quality maintenance for decentralized power supplies. The HES systems have effective short-time overload output and have efficient response characteristics in the particular [15, 16]. In this study, BFO algorithm is used to optimize the Proportional plus Integral (PI) controller gains for the load frequency control of a Two-Area Thermal Reheat Interconnected Power System (TATRIPS) in a restructured environment with and without HES unit. Various case studies are analyzed to develop Power System Ancillary Service Requirement Assessment Indices (PSASRAI) namely, Feasible Assessment Index (FAI) and Complete Assessment Index (CAI) which are able to predict the normal operating mode, emergency mode and restorative modes of the power system.

II. MODELING OF A TWO-AREA THERMAL REHEAT INTERCONNECTED POWER SYSTEM (TATRIPS) IN RESTRUCTURED SCENARIO

Even though the utilities of the power system act as monopoly in the Vertical Integrated Utility (VIU) to provide secure and relative cheap energy it has a drawback that it is an uncontrollable bureaucratic organization. The deregulation philosophy broke the monolithic power sector into distinct parts, as generators, transmission, distribution, trader, etc The traditional centralized energy generation methods are replaced or completed by distributed generation as the gas engines, energy storing devices, Photo Volatile or small hydro, etc. It poses several issues as the controllability of the net, the standardized design and operation, scale of economics, etc. The present trend is the introduction of low-energy –need technologies and the better efficiency of the usage [17, 18]. In the restructured competitive environment of power system, the Vertically Integrated Utility (VIU) no longer exists. The deregulated power system consists of GENCOs, DISCOs, Transmissions Companies (TRANSCOs) and Independent System Operator (ISO). Although it is conceptually clean to have separate functionalities for the GENCOs, TRANSCOs and DISCOs, in reality there will exist companies with combined or partial responsibilities.

With the emergence of the distinct identities of GENCOs, TRANSCOs, DISCOs and the ISO, many of the ancillary services of a VIU will have a different role to play and hence have to be modeled differently. Among these ancillary service controls one of the most important services to be enhanced is the Load-frequency control.

The LFC in a deregulated electricity market should be designed to consider different types of possible transactions, such as Poolco-based transactions, bilateral transactions and a combination of these two [7]. In the new scenario, a DISCO can contract individually with a GENCO for acquiring the power and these transactions will be made under the supervision of ISO. To make the visualization of contracts easier, the concept of "DISCO Participation Matrix" (DPM) is used which essentially provides the information about the participation of a DISCO in contract with a GENCO. In DPM, the number of rows will be equal to the number of GENCOs and the number of columns will be equal to the number of DISCOs in the system. Any entry of this matrix is a fraction of total load power contracted by a DISCO toward a GENCO. As a results total of entries of column belong to DISCOi of DPM is $\sum_i cpf_{ij} = 1$. In this study two-area interconnected power system in which each area has two GENCOs and two DISCOs. Let GENCO 1, GENCO 2, DISCO 1, DISCO 2 be in area 1 and GENCO 3, GENCO 4, DISCO 3, DISCO 4 be in area 2 as shown in Fig 1. The corresponding DPM is given as follows [4]
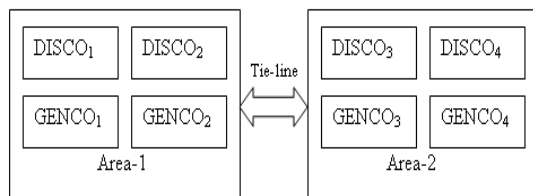

Fig .1 Schematic diagram of two-area system in restructured environment

$$DPM = \begin{bmatrix} cpf_{11} & cpf_{12} & cpf_{13} & cpf_{14} \\ cpf_{21} & cpf_{22} & cpf_{23} & cpf_{24} \\ cpf_{31} & cpf_{32} & cpf_{33} & cpf_{34} \\ cpf_{41} & cpf_{42} & cpf_{43} & cpf_{44} \end{bmatrix} \begin{matrix} G \\ E \\ N \\ C \\ O \end{matrix} \tag{1}$$

Where cpf represents "Contract Participation Factor" and is like signals that carry information as to which the GENCO has to follow the load demanded by the DISCO. The actual and scheduled steady state power flow through the tie-line are given as

$$\Delta P_{tie1-2,\,scheduled} = \sum_{i=1}^{2}\sum_{j=3}^{4} cpf_{ij}\Delta P_{L\,j} - \sum_{i=3}^{4}\sum_{j=1}^{2} cpf_{ij}\Delta P_{L\,j} \tag{2}$$

$$\Delta P_{tie1-2,\,actual} = \left(2\pi T_{12}/s \right)\left(\Delta F_1 - \Delta F_2\right) \tag{3}$$

And at any given time, the tie-line power error $\Delta P_{tie1-2,\,error}$ is defined as

$$\Delta P_{tie1-2,\,error} = \Delta P_{tie1-2,\,actual} - \Delta P_{tie1-2,\,scheduled} \tag{4}$$

The error signal is used to generate the respective ACE signals as in the traditional scenario

$$ACE_1 = \beta_1 \Delta F_1 + \Delta P_{tie\,1-2,\,error} \tag{5}$$

$$ACE_2 = \beta_2 \Delta F_2 + \Delta P_{tie\,2-1,\,error} \tag{6}$$

For two area system as shown in Fig.1, the contracted power supplied by ith GENCO is given as

$$\Delta Pg_i = \sum_{j=1}^{DISCO=4} cpf_{i\,j}\Delta PL_j \tag{7}$$

Also note that $\Delta PL_{1,LOC} = \Delta PL_1 + \Delta PL_2$ and $\Delta PL_{2,LOC} = \Delta PL_3 + \Delta PL_4$. In the proposed LFC implementation, contracted load is fed forward through the DPM matrix to GENCO set points. The actual loads affect system dynamics via the input $\Delta PL_{,LOC}$ to the power system blocks. Any mismatch between actual and contracted demands will result in frequency deviations that will drive LFC to re dispatch the GENCOs according to ACE participation factors, i.e., apf$_{11}$, apf$_{12}$, apf$_{21}$ and apf$_{22}$. The state space representation of the minimum realization model of 'N' area interconnected power system may be expressed as [19].

$$\dot{x} = Ax + Bu + \Gamma d$$
$$y = Cx \tag{8}$$

Where $x = [x_1^T, \Delta p_{ei}\ldots x_{(N-1)}^T, \Delta p_{e(N-1)}\ldots x_N^T]^T$, n - state

vector $n = \sum_{i=1}^{N} n_i + (N-1)$

$u = [u_1,\ldots u_N]^T = [\Delta P_{C1}\ldots P_{CN}]^T, N$ - Control input vector

$d = [d_1,\ldots d_N]^T = [\Delta P_{D1}\ldots P_{DN}]^T, N$ - Disturbance input vector

$y = [y_1\ldots y_N]^T, 2N$ - Measurable output vector

where A is system matrix, B is the input distribution matrix, Γ is the disturbance distribution matrix, C is the control output distribution matrix, x is the state vector, u is the control vector and d is the disturbance vector consisting of load changes.

III. HYDROGEN ENERGY STORAGE SYSTEM (HESS)

Generally the optimization of the schedule of distributed energy sources depends on the constraints of the problem which are load limits, actual generation capabilities, status of the battery, forecasted production schedule. Hydrogen is a serious contender for future energy storage due to its versatility. Consequently, producing hydrogen from renewable resources using electrolysis is currently the most desirable objective available.

A. Aqua Electrolyzer for production of Hydrogen

An aqua electrolyzer is a device that produces hydrogen and oxygen from water. Water electrolysis is a reverse process of electrochemical reaction that takes place in a fuel cell. An aqua electrolyzer converts dc electrical energy into chemical energy stored in hydrogen. From electrical circuit point of view, an aqua electrolyzer can be considered as a voltage-sensitive nonlinear dc load. For a given aqua electrolyzer, within its rating range, the higher the dc voltage applied, the larger is the load current. That is, by applying a higher dc voltage, more H_2 can be generated. In this paper, the aqua electrolyzer is considered as a subsystem which absorbs the rapidly fluctuating output power. It generates hydrogen and stores in the hydrogen tank and this hydrogen is used as fuel for the fuel cell.

B. Constant electrolyzer power

The effects of operating the electrolyzer at constant power has to be studied which is the common practice for conventional electrolysis plants. The electrolyzer and the hydrogen storage tanks are designed so that no wind energy is dissipated, and the amount of hydrogen obtained is more efficient. The electrolyzer rating is decided to be equal to [15]

$$P_e^{\max} = p_w^{\max} - P_g^{\max} - \min\left(P_i\ (t)\right) \tag{9}$$

The hydrogen storage tanks are sized according to the following criterion [15].

$$0 < V_H(t) - V_H^{\max} \qquad for \quad t = 1....N \tag{10}$$

So that the hydrogen storage does not reach the lower and upper limits during the simulation period. For each of the hydrogen-load scenarios, simulations have been run for different wind power capacities. The required hydrogen storage capacity for the different hydrogen-filling scenarios and wind power capacities have to be obtained which results in a nonlinear relationship between the required hydrogen storage and the installed wind power. It can be noted that for a fixed wind power capacity, a lower hydrogen-filling rate leads to larger hydrogen storage as with the normal operating conditions; only excess wind power is used for hydrogen production. If the hydrogen-filling rate is low, it takes longer time to reduce the hydrogen content in the storage tanks. Thus, a higher storage capacity is necessary to prevent that the

upper limit is reached. The production cost of hydrogen as a function of wind power capacity for the different hydrogen-filling scenarios. The hydrogen production cost increases rapidly, because of the extra investment in electrolyzer and especially hydrogen storage tanks needed to prevent dissipation of wind energy. All the curves of hydrogen filling scenarios reach a point where the increase in cost changes significantly. This point is chosen as the maximum preferable wind power capacity for the corresponding scenario. Hydrogen production cost increases approximately linearly with wind power capacity below this point. A part of P_{WPG} or/and P_{PV} is to be utilized by AE for the production of hydrogen to be used in fuel-cell for generation of power. The transfer function can be expressed as first order lag:

$$G_{AE}\ (s)\ =\ \frac{K_{AE}}{1 + sT_{AE}} \tag{11}$$

C. Fuel cell for energy storage

Fuel cells are static energy conversion device which converts the chemical energy of fuel (hydrogen) directly into electrical energy. They are considered to be an important resource in hybrid distributed power system due to the advantages like high efficiency, low pollution etc. An electrolyzer uses electrolysis to breakdown water into hydrogen and oxygen. The oxygen is dissipated into the atmosphere and the hydrogen is stored so it can be used for future generation. A fuel cell converts stored chemical energy, in this case hydrogen, directly into electrical energy. A fuel cell consists of two electrodes that are separated by an electrolyte as shown in Fig 2. Hydrogen is passed over the anode (negative) and oxygen is passed over the cathode (positive), causing hydrogen ions and electrons to form at the anode. The energy produced by the various types of cells depends on the operation temperature, the type of fuel cell, and the catalyst used. Fuel cells do not produce any pollutants and have no moving parts.
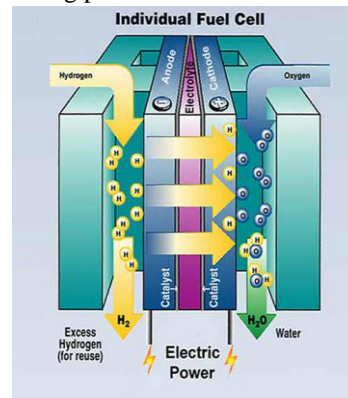

Fig 2. Structure of a fuel cell

The transfer function of Fuel Cell (FC) can be given by a simple linear equation as

$$G_{FC}(s) = \frac{K_{FC}}{1 + sT_{FC}} \qquad (12)$$

Hydrogen is one of the promising alternatives that can be used as an energy carrier. The universality of hydrogen implies that it can replace other fuels for stationary generating units for power generation in various industries. Having all the advantages of fossil fuels, hydrogen is free of harmful emissions when used with dosed amount of oxygen, thus reducing the greenhouse effect [16]. Essential elements of a hydrogen energy storage system comprise an electrolyzer unit which converts electrical energy input into hydrogen by decomposing water molecules, the hydrogen storage system itself and a hydrogen energy conversion system which converts the stored chemical energy in the hydrogen back to electrical energy as shown in fig 3. The over all transfer function of hydrogen Energy storage unit has can be

$$G_{HES}(s) = \frac{K_{HES}}{1 + sT_{HES}} = \frac{K_{AE}}{1 + sT_{AE}} * \frac{K_{FC}}{1 + sT_{FC}} \qquad (13)$$
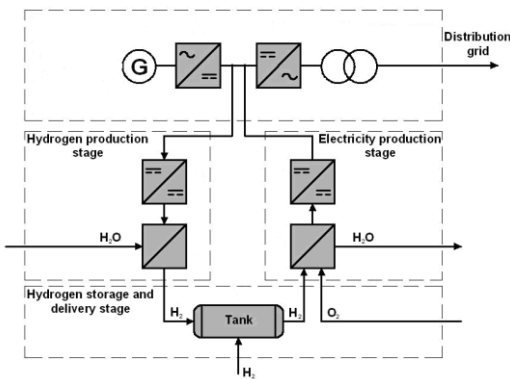

Fig 3 Block diagram of the hydrogen storage unit

D. Control design of Hydrogen Energy Storage unit
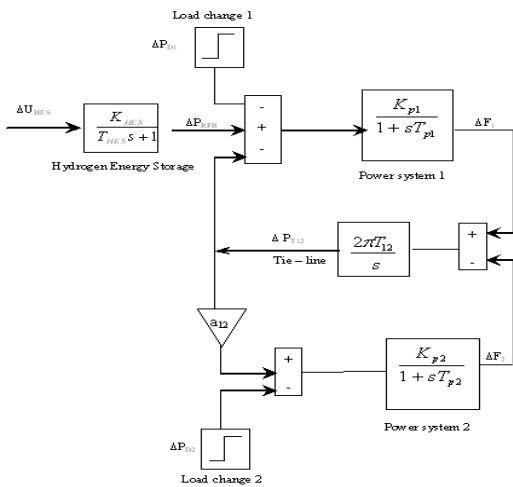

Fig. 4 Linearized reduction model for the control design

The control actions of Hydrogen Energy Storage (HES) units are found to be superior to the action of the governor system in terms of the response speed against, the frequency fluctuations [15]. The HES units are tuned to suppress the peak value of frequency deviations quickly against the sudden load change, subsequently the governor system are actuated for compensating the steady state error of the frequency deviations. Fig.4 shows the linearized reduction model for the control design of two area interconnected power system with HES units. The HES unit is modeled as an active power source to area 1 with a time constant T_{HES}, and gain constant K_{HES}. Assuming the time constants T_{HES} is regarded as 0 sec for the control design [7], then the state equation of the system represented by Fig. 4 becomes

$$\begin{bmatrix} \Delta \dot{F}_1 \\ \Delta \dot{P}_{T12} \\ \Delta \dot{F}_2 \end{bmatrix} = \begin{bmatrix} -\dfrac{1}{T_{p1}} & -\dfrac{K_{p1}}{T_{p1}} & 0 \\ 2\pi T_{12} & 0 & -2\pi T_{12} \\ 0 & \dfrac{a_{12} k_{p2}}{T_{p2}} & -\dfrac{1}{T_{p2}} \end{bmatrix} \begin{bmatrix} \Delta F_1 \\ \Delta P_{T12} \\ \Delta F_2 \end{bmatrix} + \begin{bmatrix} \dfrac{k_{p1}}{T_{p1}} \\ 0 \\ 0 \end{bmatrix} [\Delta P_{HES}] \qquad (1$$

The design process starts from the reduction of two area system into one area which represents the Inertia centre mode of the overall system. The controller of HES is designed for the equivalent one area system to reduce the frequency deviation of inertia centre. The equivalent system is derived by assuming the synchronizing coefficient T_{12} to be large.

From the state equation of $\Delta \dot{P}_{T12}$ in Eq (14)

$$\frac{\Delta \dot{P}_{T12}}{2\pi T_{12}} = \Delta F_1 - \Delta F_2 \qquad (15)$$

Setting the value of T_{12} in Eq (15) to be infinity yields $\Delta F_1 = \Delta F_2$. Next, by multiplying state equation of $\Delta \dot{F}_1$ and $\Delta \dot{F}_2$ by $\dfrac{T_{p1}}{k_{p1}}$ and $\dfrac{T_{p2}}{a_{12} k_{p2}}$ respectively, then

$$\frac{T_{p1}}{k_{p1}} \Delta \dot{F}_1 = -\frac{1}{k_{p1}} \Delta F_1 - \Delta P_{T12} + \Delta P_{HES} \qquad (16)$$

$$\frac{T_{p2}}{a_{12} k_{p2}} \Delta \dot{F}_2 = \frac{-1}{k_{p2} a_{12}} \Delta F_2 + \Delta P_{T12} \qquad (17)$$

By summing Eq (16) and Eq (17) and using the above relation $\Delta F_1 = \Delta F_2 = \Delta F$

$$\Delta \dot{F} = \frac{\left(-\dfrac{1}{k_{p1}} - \dfrac{1}{k_{p2} a_{12}} \right)}{\left(\dfrac{T_{p1}}{k_{p1}} + \dfrac{T_{p2}}{k_{p2} a_{12}} \right)} \Delta F + \frac{1}{\left(\dfrac{T_{p1}}{k_{p1}} + \dfrac{T_{p2}}{k_{p2} a_{12}} \right)} \Delta P_{HES} + C\Delta P_D \qquad (18)$$

Where ΔP_D is the load change in this system and the control $\Delta P_{HES} = -K_{HES} \Delta F$ is applied then.

$$\Delta F = \frac{C}{s + A + K_{HES} B} \Delta P_D \qquad (19)$$

Where
$$A = \left(-\frac{1}{k_{p1}} - \frac{1}{k_{p2}a_{12}} \right) \Big/ \left(\frac{T_{p1}}{k_{p1}} + \frac{T_{p2}}{k_{p2}a_{12}} \right)$$

$$B = \frac{1}{\left[\dfrac{T_{p1}}{K_{p1}} + \dfrac{T_{p2}}{K_{p2}a_{12}} \right]}$$

Where C is the proportionality constant between change in frequency and change in load demand. Since the control action of HES unit is to suppress the deviation of the frequency quickly against the sudden change of ΔP_D, the percent reduction of the final value after applying a step change ΔP_D can be given as a control specification. In Eq (19) the final values with $K_{HES} = 0$ and with $K_{HES} \neq 0$ are C/A and C/(A+K_{HES} B) respectively therefore the percentage reduction is represented by

$$C/(A + K_{HES}\ B)\Big/(C/A) = R\big/100 \qquad (20)$$

For a given R, the control gain of HES is calculated as

$$K_{HES} = \frac{A}{BR}(100 - R) \qquad (21)$$

The linearized model of an interconnected two-area reheat thermal power system in deregulated environment is shown in Fig.5 after incorporating HES unit

IV. DESIGN OF DECENTRALIZED PI CONTROLLERS

The proportional plus Integral controller gain values (K_{pi}, K_{Ii}) are tuned based on the settling time of the output response of the system (especially the frequency deviation) using Bacterial Foraging Optimization (BFO) technique. The closed loop stability of the system with decentralized PI controllers are assessed using settling time of the system output response. It is observed that the system whose output response settles fast will have minimum settling time based criterion [20] and can be expressed as

$$F(K_p, K_i) = \min(\zeta_{si}) \qquad (22)$$

$$U_1 = -K_p\ ACE_1 - K_I \int ACE_1\ dt \qquad (23)$$

$$U_2 = -K_p\ ACE_2 - K_I \int ACE_2\ dt \qquad (24)$$

Where, K_p = Proportional gain, K_I = Integral gain, ACE= Area Control Error, U_1, U_2 = Control input requirement of the respective areas, ζ_{si} = settling time of the frequency deviation of the ith area under disturbance. The relative simplicity of this controller is a successful approach towards the zero steady state error in the frequency of the system. With these optimized gain values the performance of the system is analyzed and various PSRAI are computed

V. BACTERIAL FORAGING OPTIMIZATION (BFO) TECHNIQUE

A. Review of Bacterial Foraging Optimization

The BFO method was introduced by Passino [13] motivated by the natural selection which tends to eliminate the animals with poor foraging strategies and favor those having successful foraging strategies. The foraging strategy is governed by four processes namely Chemotaxis, Swarming, Reproduction and Elimination and Dispersal. Chemotaxis process is the characteristics of movement of bacteria in search of food and consists of two processes namely swimming and tumbling. A bacterium is said to be swimming if it moves in a predefined direction, and tumbling if it starts moving in an altogether different direction. To represent a tumble, a unit length random direction $\phi(j)$ is generated. Let, "j" is the index of chemotactic step, "k" is reproduction step and "l" is the elimination dispersal event. $\theta_i(j,k,l)$, is the position of ith bacteria at j^{th} chemotactic step k^{th} reproduction step and l^{th} elimination dispersal event. The position of the bacteria in the next chemotatic step after a tumble is given by

$$\theta^i(j+1,\ k,\ l) = \theta^i(j,\ k,\ l) + C(i)\ \phi(j) \qquad (25)$$

If the health of the bacteria improves after the tumble, the bacteria will continue to swim to the same direction for the specified steps or until the health degrades. Bacteria exhibits swarm behavior i.e. healthy bacteria try to attract other bacterium so that together they reach the desired location (solution point) more rapidly. The effect of swarming [14] is to make the bacteria congregate into groups and moves as concentric patterns with high bacterial density. Mathematically swarming behavior can be modeled

$$
\begin{aligned}
J_{cc}(\theta, P(j,k,l)) &= \sum_{i=1}^{S} J^i cc\big(\theta, \theta^i(j,k,l)\big) \\
&= \sum_{i=1}^{S} \left[-d_{attract}\ \exp(-\omega_{attract}) \sum_{m=1}^{P} \big(\theta^m - \theta_m^i\big)^2 \right] \\
&+ \sum_{i=1}^{S} \left[-h_{repelent}\ \exp(-w_{repelent}) \sum_{m=1}^{P} \big(\theta^m - \theta_m^i\big)^2 \right]
\end{aligned}
\qquad (26)
$$

Where J_{CC} - Relative distance of each bacterium from the fittest bacterium, S - Number of bacteria, p - Number of parameters to be optimized, θ^m - Position of the fittest bacteria, $d_{attract}$, $\omega_{attract}$, $h_{repelent}$, $\omega_{repelent}$ - different co-efficient representing the swarming behavior of the bacteria which are to be chosen properly. In Reproduction step, population members who have sufficient nutrients will reproduce and the least healthy bacteria will die. The healthier population replaces unhealthy bacteria which get eliminated owing to their poorer foraging abilities. This makes the population of bacteria constant in the *evolution* process. In this process a sudden unforeseen event may drastically alter the evolution and may cause the elimination and / or dispersion to a new environment. Elimination and dispersal

helps in reducing the behavior of stagnation i.e., being trapped in a premature solution point or local optima.

B. Bacterial Foraging Algorithm

In case of BFO technique each bacterium is assigned with a set of variable to be optimized and are assigned with random values [Δ] within the universe of discourse defined through upper and lower limits between which the optimum value is likely to fall. In the proposed method of proportional plus integral gain (K_{Pi}, K_{Ii}) (i =1, 2) scheduling, each bacterium is allowed to take all possible values within the range and the objective function which is represented by Eq (22) is minimized. In this study, the BFO algorithm reported in [14] is found to have better convergence characteristics and is implemented as follows.

Step -1 Initialization;

1. Number of parameter (*p*) to be optimized.

2. Number of bacterial (*S*) to be used for searching the total region.

3. Swimming length (*Ns*), after which tumbling of bacteria will be undertaken in a chemotactic loop

4. N_C - the number of iteration to be undertaken in a chemotactic loop ($N_C > N_S$)

5. N_{re} - the maximum number of reproduction to be undertaken.

6. N_{ed} the maximum number of elimination and dispersal events to be imposed over bacteria

7. P_{ed} - the probability with which the elimination and dispersal events will continue.

8. The location of each bacterium *P (1-p, 1-s, 1)* which is specified by random numbers within [-1, 1]

9. The value of *C (i)*, which is assumed to be constant in this case for all bacteria to simplify the design strategy.

10. The value of $d_{attract}$, $W_{attract}$, $h_{repelent}$ and $W_{repelent}$. It is to be noted here that the value of $d_{attract}$ and $h_{repelent}$ must be same so that the penalty imposed on the cost function through "J_{CC}" of Eq (26) will be "0" when all the bacteria will have same value, i.e. they have converged.

After initialization of all the above variables, keeping one variable changing and others fixed the value of "U" is obtained by obtaining the simulation of system using the parameter contained in each bacterium. For the corresponding minimum cost, the magnitude of the changing variable is selected. Similar procedure is carried out for other variables keeping the already optimized one unchanged. In this way all the variables of step 1- initialization are obtain and are presented below

$S = 6$, $N_c = 10$, $Ns = 3$, $N_{re} = 15$, $N_{ed} = 2$, $P_{ed} = 0.25$, $d_{attract} = 0.01$, $w_{attract} = 0.04$, $h_{repelent} = 0.01$, and $w_{repelent} = 10$, $p = 2$.

Step - 2 Iterative algorithms for optimization:

This section models the bacterial population chemotaxis Swarming, reproduction, elimination, and dispersal (initially, $j=k=l= 0$) for the algorithm updating θ^i automatically results in updating of `P'.

1. Elimination –dispersal loop: $l = l + 1$

2. Reproduction loop: $k = k + 1$

3. Chemotaxis loop: $j = j + 1$

a) For i =1, 2...*S*, calculate cost for each bacterium *i* as follows. Compute value of cost $J(i, j, k, l)$ Let

$$J_{sw}(i, j, k, l) = J(i, j, k, l) + J_{cc}(\theta^i(j, k, l), P(j, k, l))$$ [i.e., add on the cell to cell attractant effect obtained through Eq (26) for swarming behavior to obtain the cost value obtained through Eq (22)].Let $J_{last} = J_{sw}(i, j, k, l)$ to save this value since a better cost via a run be found. End of for loop.

b) For *i*=1, 2….S take the tumbling / swimming decision. Tumble: generate a random vector $\Delta(i) \in \Re^p$ with each element $\Delta_m(i)$ $m = 1, 2, ...p$, a random number ranges from [-1, 1].Move the position the bacteria in the next chemotatic step after a tumble by Eq (25). Fixed step size in the direction of tumble for bacterium '*i*' is considered. Compute $J(i, j+1, k, l)$ and then let

$$J_{sw}(i, j+1, k, l) = J(i, j+1, k, l) + J_{cc}(\theta^i(j+1, k, l), P(j+1, k, l)) \quad (27)$$

Swim: Let m = 0 ;(counter for swim length), While *m<Ns* (have not climbed down too long), Let *m=m+1*, If $J_{sw}(i, j+1, k, l) < J_{last}$ (if doing better), let $J_{last} = J_{sw}(i, j+1, k, l)$ and let

$$\theta^i(j+1, \ k, \ l) = \theta^i(j, \ k, \ l) + C(i)\frac{\Delta(i)}{\sqrt{\Delta^T(i) \ \Delta(i)}} \quad (28)$$

Where $C(i)$ denotes step size; $\Delta(i)$ Random vector; $\Delta^T(i)$ Transpose of vector $\Delta(i)$ .using Eq (20) the new $J(i, j+1, k, l)$ is computed. Else let $m=N_s$ This the end of while statement

c). Go to next bacterium *(i+1)* is selected if $i \neq S$ (i.e. go to step- b) to process the next bacterium

4. If *j< N_c, go* to step 3. In this case, chemotaxis is continued since the life of the bacteria is not over.

5. Reproduction

a). For the given k and *l* for each *i=1,2…S*, let $J^i_{health} = \min_{j \in \{1...N_c\}}\{J_{sw}(i, j, k, l)\}$ be the health of the bacterium *i* (a measure of how many nutrients it got over its life time and how successful it was in avoiding noxious substance). Sort bacteria in the order of ascending cost J_{health} (higher cost means lower health).

b). when $S_r = S/2$ bacteria with highest J_{health} values die and other S_r bacteria with the best Value split [and the copies that are placed at the same location as their parent].

6. If $k<N_{re}$, go to 2; in this case, as the number of specified reproduction steps have not been reached, so the next generation in the chemotactic loop is to be started.

7. Elimination –dispersal: for *i = 1, 2... S* with probability P_{ed}, eliminates and disperses each bacterium [this keeps the number of bacteria in the population constant] to a random location on the optimization domain.

VI. SIMULATION RESULTS AND OBSERVATIONS

The Two-Area Thermal Reheat Interconnected Restructured Power System considered for the study consists of two GENCOs and two DISCOs in each area. The nominal parameters are given in Appendix. The optimal solution for the objective function expressed in eqn (22) is obtained using the frequency deviations of control areas and tie- line power changes. The gain values of HES (K_{HES}) are calculated by using Eq (21) for the given value of speed regulation coefficient (R). The gain value is of the HES is found to be $K_{HES} = 0.67$ The Proportional plus Integral controller gains (K_p K_i) are tuned with BFO algorithm by optimizing the solutions of control inputs for the various case studies as shown in Table 1 and 2. The results are obtained by MATLAB 7.01 software and 100 iterations are chosen for the convergence of the solution using BFO algorithm. These PI controllers are implemented in a Two-Area Thermal Reheat Interconnected restructured Power System with HES unit considering different utilization of capacity (K=0, 0.25, 0.5, 0.75, 1.0) and for different type of transactions. The corresponding frequency deviations Δf, tie- line power deviation ΔP_{tie} and control input deviations ΔP_c are obtained with respect to time as shown in figures 6, 7. Simulation results reveal that the proposed PI controller for the restructured power system coordinated with HES units greatly reduces the peak over shoot / under shoot of the frequency deviations and tie- line power flow deviation. And also it reduces the control input requirements and the settling time of the output responses are also reduced considerably is shown in Table 3. More over Power System Ancillary Service Requirement Assessment Indices (PSASRAI) namely, Feasible Assessment Indices (FAI) when the system is operating in a normal condition with both units in operation and Comprehensive Assessment Indices (CAI) are one or more unit outage in any area are obtained as discussed. In this study GENCO-4 in area 2 is outage are considered. From these Assessment Indices indicates the restorative measures like the magnitude of control input requirement, rate of change of control input requirement can be adjudged.

A. Feasible Restoration Indices

Scenario 1: Poolco based transaction

The optimal Proportional plus Integral (PI) controller gains are obtained for TATIPS considering various case studies for framing the Feasible Assessment Indices (FAI) which were obtained based on Area Control Error (ACE) as follows:

Case 1: In the TATRIPS considering both areas have two thermal reheat units. For Poolco based transaction, consider a case where the GENCOs in each area participate equally in LFC. For Poolco based transaction: the load change occurs only in area 1. It denotes that the load is demanded only by DISCO 1 and DISCO 2. Let the value of this load demand be 0.1 p.u MW for each of them i.e. $\Delta PL_1 = 0.1$ p.u MW, $\Delta PL_2 = 0.1$ p.u MW, $\Delta PL_3 = \Delta PL_4 = 0.0$. DISCO Participation Matrix (DPM) [7] referring to Eq (1) is considered as   [1- 4]

$$DPM = \begin{bmatrix} 0.5 & 0.5 & 0 & 0 \\ 0.5 & 0.5 & 0 & 0 \\ 0 & 0 & 0 & 0 \\ 0 & 0 & 0 & 0 \end{bmatrix} \qquad (29)$$

Note that DISCO 3 and DISCO 4 do not demand power from any of the GENCOs and hence the corresponding contract participation factors (columns 3 and 4) are zero. DISCO 1 and DISCO 2 demand identically from their local GENCOs, viz., GENCO 1 and GENCO 2. Therefore, $cpf_{11} = cpf_{12} = 0.5$ and $cpf_{21} = cpf_{22} = 0.5$. The frequency deviations (ΔF) of area, tie-line power deviation (ΔP_{tie}) and control input requirements deviations (ΔP_c) of both areas are as shown the Fig 6. The settling time (ς_s) and peak over /under shoot (Mp) of the control input deviations (ΔP_c) in both the area were obtained from Fig 6. From the Fig 6 (d) and (e) the corresponding Feasible Assessment Indices FAI_1, FAI_2, FAI_3 and FAI_4 are calculated as follows

Step 6.1 The Feasible Assessment Index 1 (ε_1) is obtained from the ratio between the settling time of the control input deviation $\Delta P_{c1}(\varsigma_{s1})$ response of area 1 and power system time constant (T_{p1}) of area 1

$$FRI_1 = \frac{\Delta P_{c1}(\varsigma_{s1})}{T_{p1}} \qquad (30)$$

Step 6.2 The Feasible Assessment Index 2 (ε_2) is obtained from the ratio between the settling time of the control input deviation $\Delta P_{c2}(\varsigma_{s2})$ response of area 2 and power system time constant (T_{p2}) of area 2

$$FRI_2 = \frac{\Delta P_{c2}(\varsigma_{s2})}{T_{p2}} \qquad (31)$$

Step 6.3 The Feasible Assessment Index 3 (ε_3) is obtained from the peak value of the control input deviation $\Delta P_{c1}(\varsigma_p)$ response of area 1 with respect to the final value $\Delta P_{c1}(\varsigma_s)$

$$FRI_3 = \Delta P_{c1}(\varsigma_p) - \Delta P_{c1}(\varsigma_s) \qquad (32)$$

Step 6.4 The Feasible Assessment Index 4 (ε_4) is obtained from the peak value of the control input deviation $\Delta P_{c2}(\varsigma_p)$ response of area 1 with respect to the final value $\Delta P_{c2}(\varsigma_s)$

$$FRI_4 = \Delta P_{c2}(\varsigma_p) - \Delta P_{c2}(\varsigma_s) \qquad (33)$$

Case 2: This case is also referred a Poolco based transaction on TATRIPS where in the GENCOs in each area participate not equally in LFC and load demand is more than the GENCO in area 1 and the load demand change occurs only in area 1. This condition is indicated in the column entries of the DPM matrix and sum of the column entries is more than unity.

Case 3: It may happen that a DISCO violates a contract by demanding more power than that specified in the contract and this excess power is not contracted to any of the GENCOs. This uncontracted power must be supplied by the GENCOs in the same area to the DISCO. It is represented as a local load of the area but not as the contract demand. Consider scenario-1 again with a modification that DISCO 1 demands 0.1 p.u MW of excess power i.e., $\Delta Puc_{,1} = 0.1$ p.u MW and $\Delta Puc_{,2} = 0.0$ p.u MW. The total load in area 1 = Load of DISCO 1+Load of DISCO 2 = $\Delta PL_1 + \Delta Puc_1 + \Delta PL_2 = 0.1 + 0.1 + 0.1 = 0.3$ p.u MW.

Case 4: This case is similar to Case 2 to with a modification that DISCO 3 demands 0.1 p.u MW of excess power i.e., $\Delta Puc_{,2} = 0.1$ p.u MW and., $\Delta Puc_{,1} = 0$ p.u MW. The total load in area 2 = Load of DISCO 3+Load of DISCO 4 = $\Delta PL_1 + \Delta PL_2 + \Delta Puc_2 = 0 + 0 + 0.1 = 0.1$ p.u MW.

Case 5: In this case which is similar to Case 2 with a modification that DISCO 1 and DISCO 3 demands 0.1 p.u MW of excess power i.e., $\Delta Puc_{,1} = 0.1$ p.u MW and $\Delta Puc_{,2} = 0.1$ p.u MW. The total load in area 1 = Load of DISCO 1+Load of DISCO 2 = $\Delta PL_1 + \Delta Puc_1 + \Delta PL_2 = 0.1 + 0.1 + 0.1 = 0.3$ p.u MW and total demand in area 2 = Load of DISCO 3+Load of DISCO 4 = $\Delta PL_3 + \Delta Puc_2 + \Delta PL_4 = 0 + 0.1 + 0 = 0.1$ p.u MW

Scenario 2: Bilateral transaction

Case 6: Here all the DISCOs have contract with the GENCOs and the following DISCO Participation Matrix (DPM) be considered [7].

$$DPM = \begin{bmatrix} 0.4 & 0.25 & 0.2 & 0.4 \\ 0.3 & 0.15 & 0.1 & 0.2 \\ 0.1 & 0.4 & 0.3 & 0.25 \\ 0.2 & 0.2 & 0.4 & 0.15 \end{bmatrix} \qquad (34)$$

In this case, the DISCO 1, DISCO 2, DISCO 3 and DISCO 4, demands 0.15 p.u MW, 0.05 p.u MW, 0.15 p.u MW and 0.05 p.u MW from GENCOs as defined by cpf in the DPM matrix and each GENCO participates in LFC as defined by the following ACE participation factor $apf_{11} = apf_{12} = 0.5$ and $apf_{21} = apf_{22} = 0.5$. The dynamic responses are shown in Fig. 7. From this Fig 7 the corresponding FAI_1, FAI_2, FAI_3 and FAI_4 are calculated.

Case 7: For this case also bilateral transaction on TATRIPS is considered with a modification that the GENCOs in each area participate not equally in LFC and load demand is more than the GENCO in both the areas. But it is assumed that the load demand change occurs in both areas and the sum of the column entries of the DPM matrix is more than unity.

Case 8: Considering in the case 7 again with a modification that DISCO 1 demands 0.1 p.u MW of excess power i.e., $\Delta Puc_{1} = 0.1$ p.u.MW and $\Delta Puc_{2} = 0.0$ p.u MW. The total load in area 1 = Load of DISCO 1+Load of DISCO 2 = $\Delta PL_1 + \Delta Puc_1 + \Delta PL_2 = 0.15 + 0.1 + 0.05 = 0.3$ p.u MW and total load in area 2 = Load of DISCO 3+Load of DISCO 4 = $\Delta PL_3 + \Delta PL_4 = 0.15 + 0.05 = 0.2$ p.u MW

Case 9: In the case which similar to case 7 with a modification that DISCO 3 demands 0.1 p.u.MW of excess power i.e., $\Delta Puc_{,2} = 0.1$ p.u MW. The total load in area 1 = Load of DISCO 1+Load of DISCO 2 = $\Delta PL_1 + \Delta PL_4 = 0.15 + 0.05 = 0.2$ p.u.MW and total demand in area 2 = Load of DISCO 3+Load of DISCO 4 = $\Delta PL_3 + \Delta PL_4 + \Delta Puc_3 = 0.15 + 0.05 + 0.1 = 0.3$ p.u MW

Case 10: In the case which similar to case 7 with a modification that DISCO 1 and DISCO 3 demands 0.1 p.u MW of excess power i.e., $\Delta Puc_{,1} = 0.1$ p.u MW and $\Delta Puc_{,2} = 0.1$ p.u MW. The total load in area 1 = Load of DISCO 1 + Load of DISCO 2 = $\Delta PL_1 + \Delta Puc_1 + \Delta PL_2 = 0.15 + 0.1 + 0.05 = 0.3$ p.u MW and total load in area 2 = Load of DISCO 3 + Load of DISCO 4 = $\Delta PL_3 + \Delta Puc_3 + \Delta PL_4 = 0.15 + 0.1 + 0.05 = 0.3$ p.u MW. For the Cases 1-10, Feasible Assessment Indices (FAI_1, FAI_2, FAI_3, and FAI_4) or $\varepsilon_{1,}$ $\varepsilon_2, \varepsilon_3$ and ε_4 are calculated are tabulated in Table 4.

B. Comprehensive Assessment Indices

Apart from the normal operating condition of the TATRIPS few other case studies like one unit outage in an area, outage of one distributed generation in an area are considered individually. With the various case studies and based on their optimal gains the corresponding CAI is obtained as follows.

Case 11: In the TATRIPS considering all the DISCOs have contract with the GENCOs but GENCO4 is outage in area-2. In this case, the DISCO 1, DISCO 2, DISCO 3 and DISCO 4, demands 0.15 p.u MW, 0.05 p.u MW, 0.15 pu.MW and 0.05 pu.MW from GENCOs as defined by cpf in the DPM matrix (26). The output GENCO4 = 0.0 p.u MW.

Case 12: Consider in this case which is same as Case 11 but DISCO 1 demands 0.1 p.u MW of excess power i.e., $\Delta Puc_{1} = 0.1$ p.u.MW and $\Delta Puc_{2} = 0.0$ p.u MW. The total load in area 1 = Load of DISCO 1+Load of DISCO 2 = $\Delta PL_1 + \Delta Puc_1 + \Delta PL_2 = 0.15 + 0.1 + 0.05 = 0.3$ p.u MW and total load in area 2 = Load of DISCO 3+Load of DISCO 4 = $\Delta PL_3 + \Delta PL_4 = 0.15 + 0.05 = 0.2$ p.u MW.

Case 13: This case is same as Case 11 with a modification that DISCO 3 demands 0.1 p.u MW of excess power i.e., $\Delta Puc_{3} = 0.1$ p.u MW. The total load in area 1 = Load of DISCO 1+Load of DISCO 2 = $\Delta PL_3 + \Delta PL_4 = 0.15 + 0.05 = 0.2$ p.u MW and total demand in area 2 = Load of DISCO 3+Load of DISCO 4 = $\Delta PL_3 + \Delta PL_4 + \Delta Puc_3 = 0.15 + 0.05 + 0.1 = 0.3$ p.u MW

Case 14: In this case which is similar to Case 11 with a modification that DISCO 1 and DISCO 3 demands 0.1 p.u MW of excess power i.e., $\Delta Puc_{1} = 0.1$ p.u.MW and $\Delta Puc_{3} = 0.1$ p.u MW. The total load in area 1 = Load of DISCO 1+Load of DISCO 2 = $\Delta PL_1 + \Delta Puc_1 + \Delta PL_2 = 0.15 + 0.1 + 0.05 = 0.3$ p.u MW and total load in area 2 = Load of DISCO 3+Load of DISCO 4 = $\Delta PL_3 + \Delta Puc_3 + \Delta PL_4 = 0.15 + 0.1 + 0.05 = 0.3$ p.u MW. For the Case 11-14, the corresponding Assessment Indices are referred as Comprehensive Assessment Indices (CAI_1, CAI_2, CAI_3, and CAI_4) are

obtained using Eq (30 to 33) as $\varepsilon_5, \varepsilon_6, \varepsilon_7 \ and \ \varepsilon_8$ and $\int P$ is the ancillary service requirement for various case studies and

A. Power System Ancillary Service Requirement Assessment Indices (PSASRAI)

a) Based on Settling Time

(i)If $\varepsilon_1, \varepsilon_2, \varepsilon_5, \varepsilon_6 \geq 1$ then the integral controller gain of each control area has to be increased causing the speed changer valve to open up widely. Thus the speed- changer position attains a constant value only when the frequency error is reduced to zero.

(ii) If $1.0 < \varepsilon_1, \varepsilon_2, \varepsilon_5, \varepsilon_6 \leq 1.5$ then more amount of distributed generation requirement is needed. Energy storage is an attractive option to augment demand side management implementation by ensuring the Ancillary Services to the power system.

(iii) If $\varepsilon_1, \varepsilon_2, \varepsilon_5, \varepsilon_6 \geq 1.5$ then the system is vulnerable and the system becomes unstable and may even result to blackouts.

b) Based on peak undershoot

are shown in Table 5.

(i)If $0.15 \leq \varepsilon_3, \varepsilon_4, \varepsilon_7, \varepsilon_8 < 0.2$ then Energy Storage Systems (ESS) for LFC is required as the conventional load-frequency controller may no longer be able to attenuate the large frequency oscillation due to the slow response of the governor for unpredictable load variations. A fast-acting energy storage system in addition to the kinetic energy of the generator rotors is advisable to damp out the frequency oscillations.

(ii) If $0.2 \leq \varepsilon_3, \varepsilon_4, \varepsilon_7, \varepsilon_8 < 0.3$ then more amount of distribution generation requirement is required or Energy Storage Systems (ESS) coordinated control with the FACTS devices are required for the improvement relatively stability of the power system in the LFC application and the load shedding is also preferable

(iii)If $\varepsilon_3, \varepsilon_4, \varepsilon_7, \varepsilon_8 > 0.3$ then the system is vulnerable and the system becomes unstable and may result to blackout.
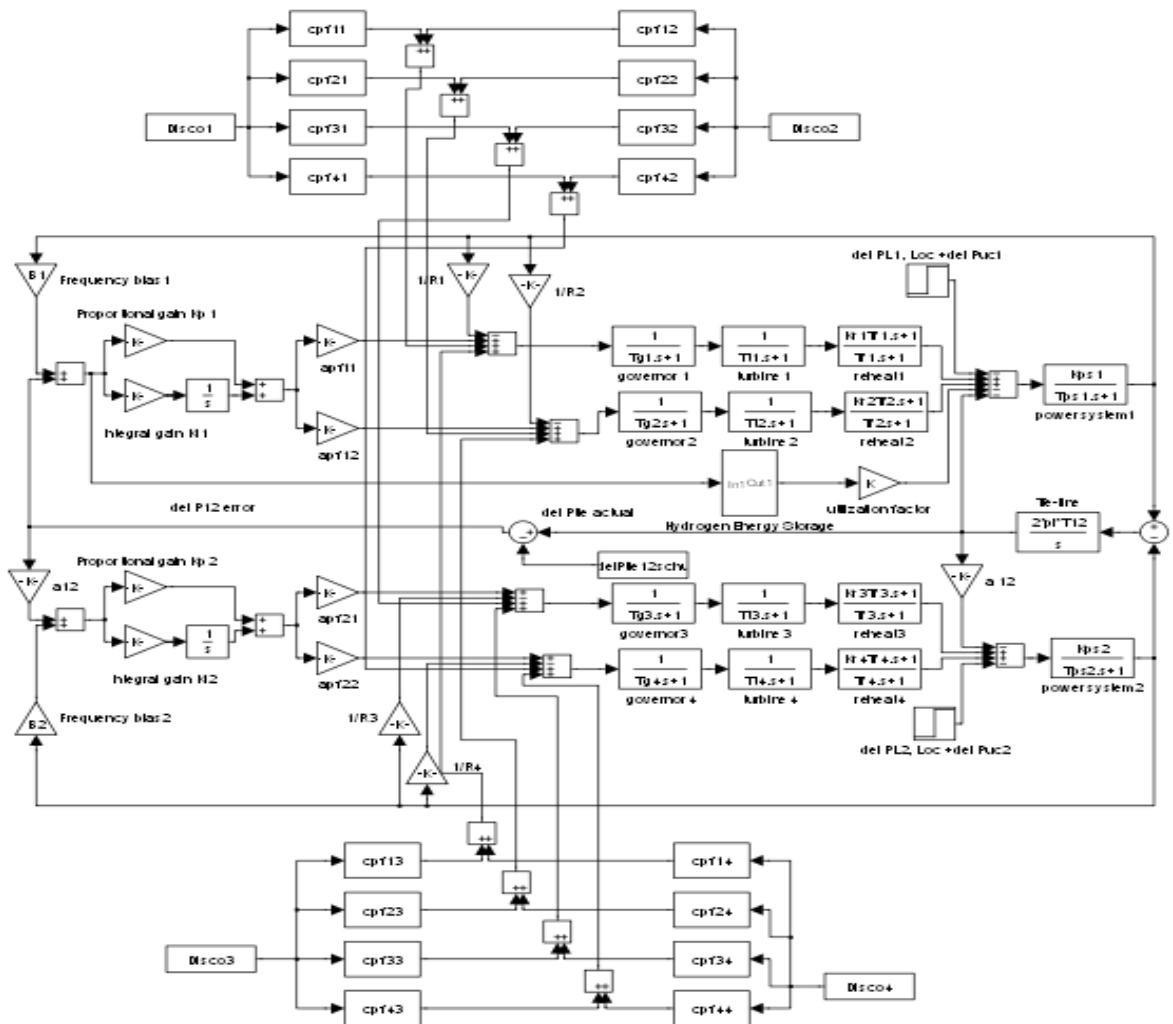

Fig. 5 Simulink model of a Two- Area Thermal Reheat Interconnected Power System (TATRIPS) in restructured environment with Hydrogen Energy Storage unit.
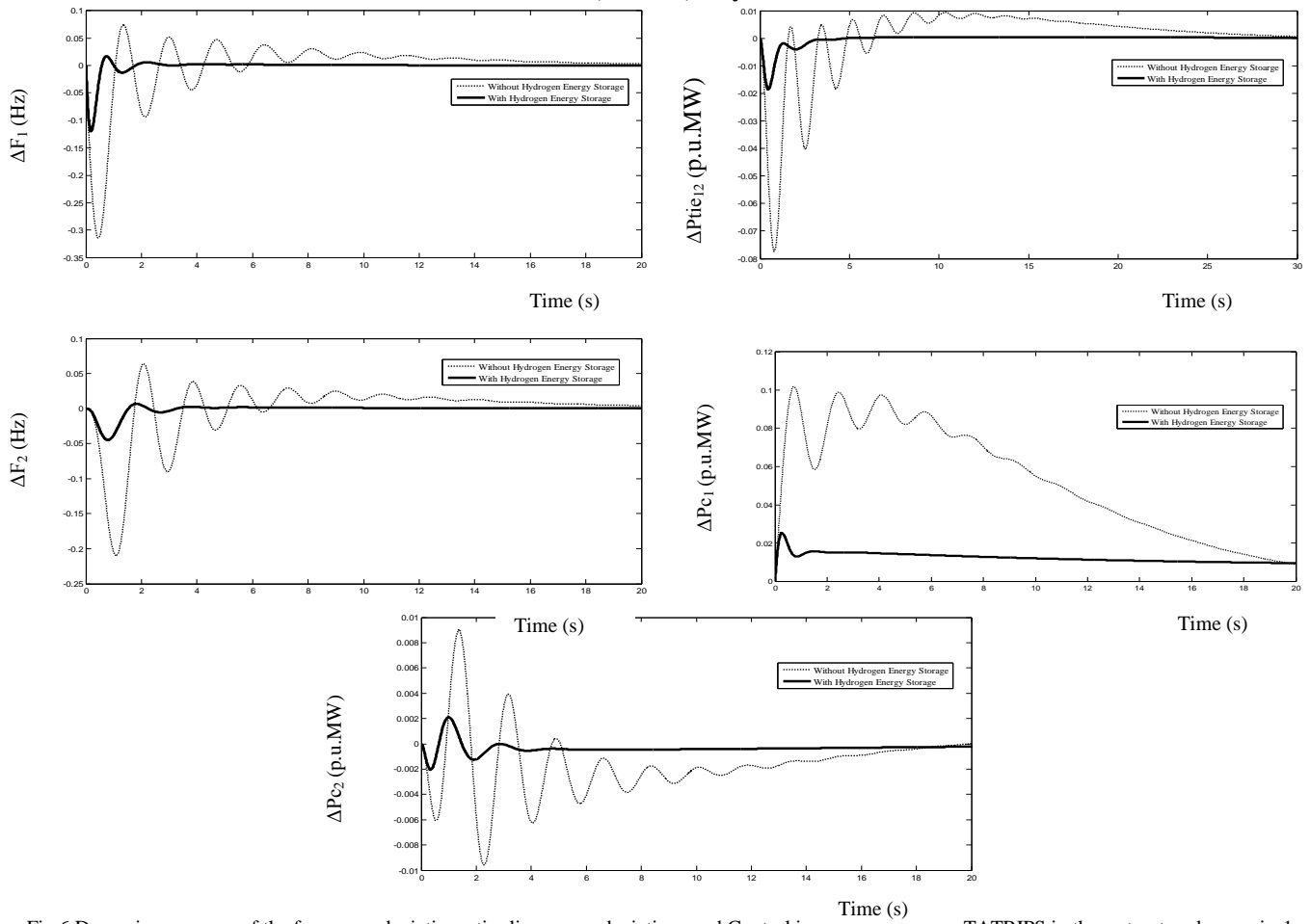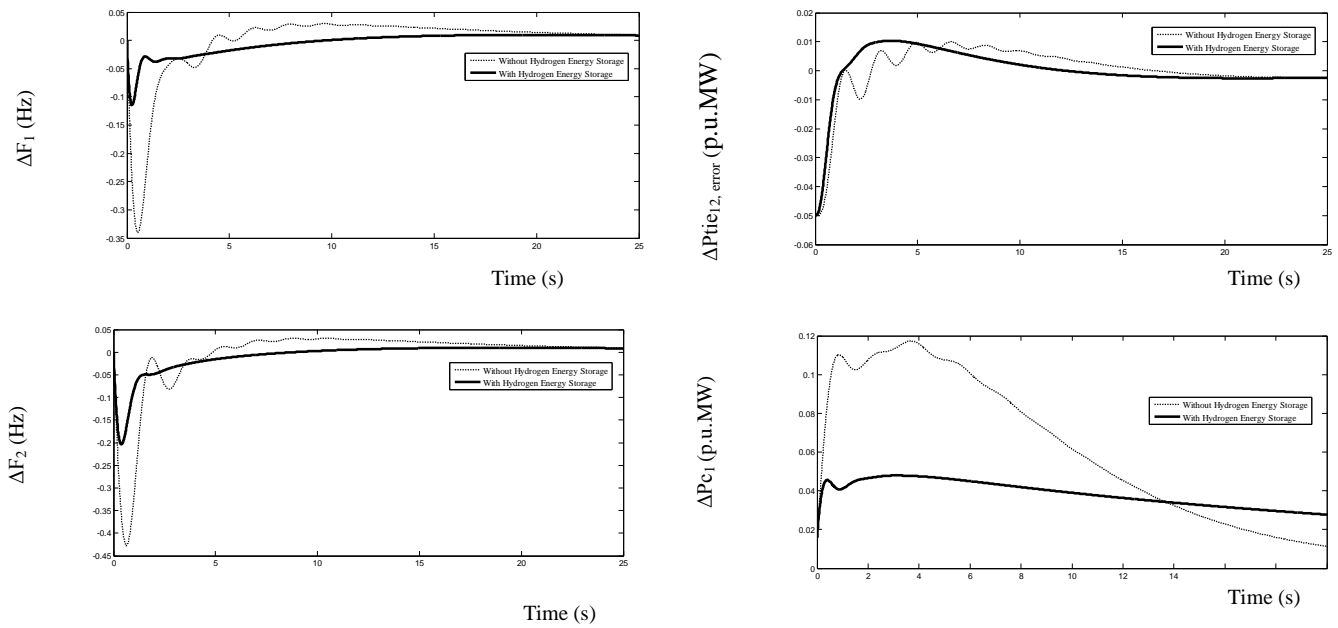
Fig.6 Dynamic responses of the frequency deviations, tie- line power deviations and Control input deviations for TATRIPS in the restructured scenario-1 (poolco based transactions)
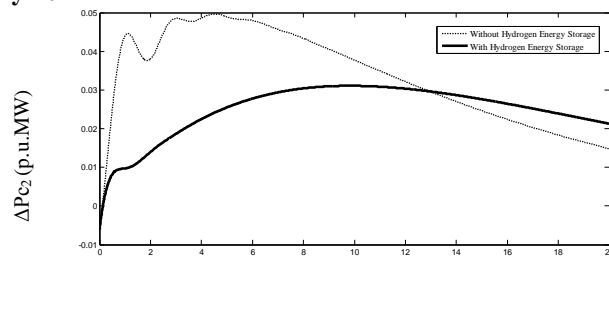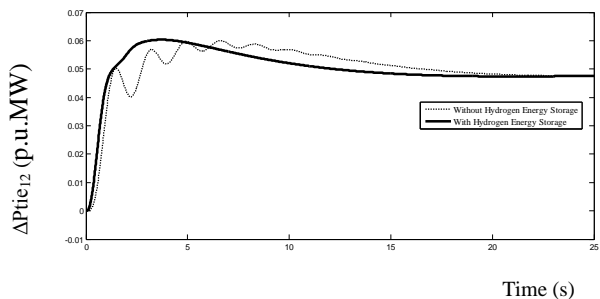
Fig.7 Dynamic responses of the frequency deviations, tie- line power deviations, and Control input deviations for TAT restructured scenario-2 (bilateral based transactions)

TATRIPS	Feasible Assessment Indices (FAI) based on control input deviations (ΔP_c) without HES unit (utilization factor K=0)					Feasible Assessment Indices (FAI) based on control input deviations (ΔP_c) with HES unit (utilization factor K=1)				
	ε_1	ε_2	ε_3	ε_4	$\int P_{without\ HES}$	ε_1	ε_2	ε_3	ε_4	$\int P_{HES}$
Case 1	0.975	0.886	0.133	0.027	1.056	0.804	0.711	0.091	0.007	0.534
Case 2	1.086	0.967	0.212	0.031	1.284	0.807	0.784	0.101	0.009	0.564
Case 3	1.326	1.025	0.297	0.045	3.262	0.814	0.901	0.125	0.011	0.591
Case 4	1.185	1.322	0.224	0.067	0.782	0.925	0.929	0.129	0.015	0.596
Case 5	1.461	1.375	0.302	0.085	3.947	1.032	1.074	0.229	0.042	0.462
Case 6	0.926	0.875	0.148	0.095	1.261	0.801	0.701	0.104	0.055	0.486
Case 7	1.126	0.916	0.216	0.098	1.452	0.887	0.896	0.142	0.071	0.531
Case 8	1.325	1.025	0.326	0.101	3.499	0.912	0.958	0.201	0.079	0.562
Case 9	1.234	1.327	0.215	0.184	1.031	0.852	1.042	0.162	0.144	0.608
Case 10	1.376	1.345	0.341	0.196	3.269	1.004	1.104	0.271	0.158	0.628

TABLE IV (a) Feasible Assessment Indices (FAI) without and with HES unit (utilization factor K=1) for TATRIPS

TATRIPS	Feasible Assessment Indices (FAI) based on control input deviations (ΔP_c) without HES unit (utilization factor K=0)					Feasible Assessment Indices (FAI) based on control input deviations (ΔP_c) with HES unit (utilization factor K=0.75)				
	ε_1	ε_2	ε_3	ε_4	$\int P_{without\ HES}$	ε_1	ε_2	ε_3	ε_4	$\int P_{HES}$
Case 1	**0.975**	**0.886**	**0.133**	**0.027**	**1.056**	**0.872**	**0.801**	**0.102**	**0.011**	**0.465**
Case 2	**1.086**	**0.967**	**0.212**	**0.031**	**1.284**	**0.881**	**0.814**	**0.123**	**0.012**	**0.471**
Case 3	**1.326**	**1.025**	**0.297**	**0.045**	**3.262**	**0.882**	**0.921**	**0.134**	**0.015**	**0.531**
Case 4	**1.185**	**1.322**	**0.224**	**0.067**	**0.782**	**0.968**	**0.982**	**0.141**	**0.019**	**0.562**
Case 5	**1.461**	**1.375**	**0.302**	**0.085**	**3.947**	**1.204**	**1.109**	**0.254**	**0.045**	**0.454**
Case 6	**0.926**	**0.875**	**0.148**	**0.095**	**1.261**	**0.808**	**0.781**	**0.121**	**0.055**	**0.472**
Case 7	**1.126**	**0.916**	**0.216**	**0.098**	**1.452**	**0.934**	**0.884**	**0.159**	**0.074**	**0.533**
Case 8	**1.325**	**1.025**	**0.326**	**0.101**	**3.499**	**0.947**	**0.942**	**0.213**	**0.082**	**0.521**
Case 9	**1.234**	**1.327**	**0.215**	**0.184**	**1.031**	**0.947**	**1.051**	**0.182**	**0.152**	**0.558**
Case 10	**1.376**	**1.345**	**0.341**	**0.196**	**3.269**	**1.101**	**1.124**	**0.283**	**0.159**	**0.591**

TABLE IV (b) Feasible Assessment Indices (FAI) without and with HES unit (utilization factor K=0.75) for TATRIPS

TATRIPS	Feasible Assessment Indices (FAI) based on control i input deviations (ΔP_c) without HES unit (utilization factor K=0)					Feasible Assessment Indices (FAI) based on control input deviations (ΔP_c) with HES unit (utilization factor K=0.25)				
	ε_1	ε_2	ε_3	ε_4	$\int P_{without\,HES}$	ε_1	ε_2	ε_3	ε_4	$\int P_{HES}$
Case 1	0.975	0.886	0.133	0.027	1.056	0.859	0.785	0.111	0.015	0.398
Case 2	1.086	0.967	0.212	0.031	1.284	0.901	0.822	0.149	0.017	0.416
Case 3	1.326	1.025	0.297	0.045	3.262	0.952	0.918	0.188	0.026	0.428
Case 4	1.185	1.322	0.224	0.067	0.782	0.962	0.954	0.151	0.041	0.526
Case 5	1.461	1.375	0.302	0.085	3.947	1.294	1.138	0.264	0.062	0.398
Case 6	0.926	0.875	0.148	0.095	1.261	0.811	0.801	0.133	0.069	0.442
Case 7	1.126	0.916	0.216	0.098	1.452	0.945	0.881	0.178	0.084	0.461
Case 8	1.325	1.025	0.326	0.101	3.499	0.958	0.962	0.258	0.089	0.445
Case 9	1.234	1.327	0.215	0.184	1.031	0.938	1.111	0.187	0.173	0.495
Case 10	1.376	1.345	0.341	0.196	3.269	1.201	1.158	0.292	0.181	0.498

TABLE IV(c) Feasible Assessment Indices (FAI) without and with HES unit (utilization factor K=0.5) for TATRIPS

TATRIPS	Feasible Assessment Indices (FAI) based on control input deviations (ΔP_c) without HES unit (utilization factor K=0)					Feasible Assessment Indices (FAI) based on control input deviations (ΔP_c) with HES unit (utilization factor K=0.5)				
	ε_1	ε_2	ε_3	ε_4	$\int P_{without\,HES}$	ε_1	ε_2	ε_3	ε_4	$\int P_{HES}$
Case 1	0.975	0.886	0.133	0.027	1.056	0.871	0.782	0.101	0.011	0.436
Case 2	1.086	0.967	0.212	0.031	1.284	0.888	0.811	0.129	0.020	0.451
Case 3	1.326	1.025	0.297	0.045	3.262	0.901	0.921	0.141	0.021	0.523
Case 4	1.185	1.322	0.224	0.067	0.782	0.958	0.953	0.151	0.023	0.542
Case 5	1.461	1.375	0.302	0.085	3.947	1.181	1.102	0.262	0.055	0.445
Case 6	0.926	0.875	0.148	0.095	1.261	0.801	0.778	0.125	0.064	0.464
Case 7	1.126	0.916	0.216	0.098	1.452	0.932	0.881	0.169	0.079	0.491
Case 8	1.325	1.025	0.326	0.101	3.499	0.942	0.962	0.232	0.082	0.471
Case 9	1.234	1.327	0.215	0.184	1.031	0.931	1.112	0.181	0.161	0.538
Case 10	1.376	1.345	0.341	0.196	3.269	1.101	1.131	0.291	0.165	0.549

TABLE IV (d) Feasible Assessment Indices (FAI) without and with HES unit (utilization factor K=0.25) for TATRIPS

TATRIPS	Comprehensive Assessment Indices (CAI) based on control input deviations (ΔP_c) without HES unit (utilization factor K=0)					Comprehensive Assessment Indices (CAI) based on control input deviations (ΔP_c) with HES unit (utilization factor K=1)				
	ε_5	ε_6	ε_7	ε_8	$\int P_{without\,HES}$	ε_5	ε_6	ε_7	ε_8	$\int P_{HES}$
Case 11	1.134	1.517	0.346	0.298	1.103	1.001	1.238	0.301	0.236	0.499
Case 12	1.524	1.524	0.383	0.341	3.194	1.083	1.344	0.311	0.301	0.595
Case 13	1.345	1.623	0.432	0.496	1.894	1.002	1.419	0.372	0.419	0.573
Case 14	1.627	1.735	0.457	0.512	3.271	1.428	1.552	0.388	0.478	0.589

TABLE V (a) Comprehensive Assessment Indices (CAI) without and with HES unit (utilization factor K=1) for TATRIPS

TATRIPS	Comprehensive Assessment Indices (CAI) based on control input deviations (ΔP_c) without HES unit (utilization factor K=0)					Comprehensive Assessment Indices (CAI) based on control input deviations (ΔP_c) with HES unit (utilization factor K=0.75)				
	ε_5	ε_6	ε_7	ε_8	$\int P_{without\,HES}$	ε_5	ε_6	ε_7	ε_8	$\int P_{HES}$
Case 11	1.134	1.517	0.346	0.298	1.103	1.024	1.333	0.306	0.244	0.448
Case 12	1.524	1.524	0.383	0.341	3.194	1.101	1.411	0.321	0.306	0.529
Case 13	1.345	1.623	0.432	0.496	1.894	1.012	1.500	0.379	0.411	0.542
Case 14	1.627	1.735	0.457	0.512	3.271	1.438	1.602	0.400	0.485	0.548

TABLE V (b) Comprehensive Assessment Indices (CAI) without and with HES unit (utilization factor =0.75) for TATRIPS

TABLE V(c) Comprehensive Assessment Indices (CAI) without and with HES unit (utilization factor K=0.5) for TATRIPS

TATRIPS	Comprehensive Assessment Indices (CAI) based on control input deviations (ΔP_c) without HES unit (utilization factor K=0)					Comprehensive Assessment Indices (CAI) based on control input deviations (ΔP_c) with HES unit (utilization factor K=0.5)				
	ε_5	ε_6	ε_7	ε_8	$\int P_{without\ HES}$	ε_5	ε_6	ε_7	ε_8	$\int P_{HES}$
Case 11	1.134	1.517	0.346	0.298	1.103	1.049	1.313	0.314	0.251	0.386
Case 12	1.524	1.524	0.383	0.341	3.194	1.191	1.422	0.322	0.311	0.449
Case 13	1.345	1.623	0.432	0.496	1.894	1.081	1.541	0.400	0.423	0.328
Case 14	1.627	1.735	0.457	0.512	3.271	1.479	1.612	0.405	0.493	0.469

TABLE V (d) Comprehensive Assessment Indices (CAI) without and with HES unit (utilization factor K=0.25) for TATRIPS

TATRIPS	Comprehensive Assessment Indices (CAI) based on control input deviations (ΔP_c) without HES unit (utilization factor K=0)					Comprehensive Assessment Indices (CAI) based on control input deviations (ΔP_c) with HES unit (utilization factor K=0.25)				
	ε_5	ε_6	ε_7	ε_8	$\int P_{without\ HES}$	ε_5	ε_6	ε_7	ε_8	$\int P_{HES}$
Case 11	1.134	1.517	0.346	0.298	1.103	1.067	1.209	0.322	0.261	0.349
Case 12	1.524	1.524	0.383	0.341	3.194	1.141	1.285	0.329	0.308	0.421
Case 13	1.345	1.623	0.432	0.496	1.894	1.149	1.452	0.401	0.432	0.439
Case 14	1.627	1.735	0.457	0.512	3.271	1.342	1.531	0.416	0.498	0.446

VII. CONCLUSION

This paper proposes the design of various Power System Ancillary Service Requirement Assessment Indices (PSASRAI) which highlights the necessary requirements to be adopted in minimizing the frequency deviations, tie-line power deviation in a two-area Thermal reheat interconnected restructured power system in a faster manner to ensure the reliable operation of the power system. The PI controllers are designed using BFO algorithm and implemented in a TATRIPS without and with HES unit. This BFO Algorithm was employed to achieve the optimal parameters of gain values of the various combined control strategies as BFO algorithm is easy to implement without additional computational complexity, with quite promising results and ability to jump out the local optima. Moreover, Power flow control by HES unit is also found to be efficient and effective for improving the dynamic performance of load frequency control of the interconnected power system than that of the system without HES unit. From the simulated results it is observed that the restoration indices calculated for the TATRIPS with HES unit indicates that more sophisticated control for a better restoration of the power system output responses and to ensure improved Power System Ancillary Service Requirement Assessment Indices (PSASRAI) in order to provide good margin of stability than that of the TATRIPS without HES unit.

ACKNOWLEDGMENT

REFERENCES

[1] Mukta, Balwinder Singh Surjan, "Load Frequency Control of Interconnected Power System in Deregulated Environment: A Literature Review", International Journal of Engineering and Advanced Technology (IJEAT) ISSN: 2249 – 8958, Vol. 2, Issue-3, pp. 435-441, 2013.

[2] Sinha S.K., Prasad R., Patel R.N., "Automatic Generation Control of restructured Power System with combined intelligent techniques", International Journal of Bio-Inspired Computation, Vol. 2, No.2, pp. 124-131, 2013.

[3] F.Liu, Y.H.Song, J.Ma, S.Mei, Q.Lu, "Optimal load-Frequency control in restructured power systems", IEE proceeding on Generation Transmission and Distribution, Vol. 150, No.1, pp. 87-95, 2003.

[4] S. Farook, P. Sangameswara Raju "AGC controllers to optimize LFC regulation in deregulated power system", International Journal of Advances in Engineering &Technology Vol. 1, Issue-5, pp. 278-289, 2011.

[5] Bevrani H, Mitani Y, Tsuji K., "Robust decentralized AGC in a restructured power system", Energy Conversion and Management, Vol. 45, pp.2297-2312, 2004

[6] V.Donde, M.A.Pai, I.A.Hiskens, Simulation and Optimization in an AGC System after Deregulation, IEEE Transactions of Power System, Vol. 16, No.3, pp.481-489, 2001.

[7] I.A.Chidambaram and B.Paramasivam, "Optimized Load-Frequency Simulation in Restructured Power System with Redox Flow Batteries and Interline Power Flow Controller", International Journal of Electrical Power and Energy Systems, Vol.50, pp 9-24, Feb 2013.

[8] Y.L. Karnavas, K.S. Dedousis, "Overall performance evaluation of evolutionary designed conventional AGC controllers for interconnected electric power system studies in deregulated market environment", International Journal

of Engineering, Science and Technology,Vol.2, No.3, pp 150-166, Feb 2010.

[9] Tan Wen, Zhang. H, Yu.M, "Decentralized load frequency control in deregulated environments", Electrical Power and Energy Systems Vol.41, pp.16-26, 2012.

[10] J.O.P.Rahi, Harish Kumar Thakur, Abhash Kumar Singh, Shashi Kant Gupta, "Ancillary Services in Restructured Environment of Power System", International Journal of Innovative Technology and Research (IJITR) ISSN: 2320–5547, Vol. 1, Issue No. 3, pp.218-225, 2013.

[11] Elyas Rakhshani,, Javad Sadesh "Practical viewpointsd on load frequency control problem in a deregulated power system", Energy Conversion and Management, Vol. 51, No. 5, pp.1148 -1156, 2010.

[12] D. Saxena, S.N. Singh, K.S. Verma, "Application of computational intelligence in emerging power systems", International Journal of Engineering, Science and Technology,Vol.2, No.3, pp 1-7, 2010.

[13] K.M.Passino, "Biomimicry of bacterial foraging for distributed optimization and control", IEEE Control Syst Magazine, Vol.22, No.3, pp. 52-67, 2002.

[14] Janardan Nanda, Mishra.S., Lalit Chandra Saikia, "Maiden Application of Bacterial Foraging-Based optimization technique in multi-area Automatic Generation Control", IEEE Transaction on Power System, Vol.24, No.2, pp. 602-609, 2009.

[15] Dimitris Ipsakis, Spyros Voutetakis, Panos Seferlisa, Fotis Stergiopoulos and Costas Elmasides, "Power management strategies for a stand-alone power system using renewable energy sources and hydrogen storage", International Journal of Hydrogen Energy Vol.34, pp 7081-7095, 2009.

[16] Ke´louwani S, Agbossou K, Chahine R, "Model for energy conversion in renewable energy system with hydrogen storage", Journal of Power Sources Vol.140, pp.392–399, 2005.

[17] Peter Kadar, "Application of Optimization Techniques in the Power System Control", ACTA Polytechnica Hungarica, Vol.10, No.5, pp.221-236, 2013. .

[18] Vijay Rohilla, K.P. Singh Parmar, Sanju Saini, "Optimization of AGC Parameters in the Restructured Power System Environment Using GA", International Journal of Engineering Sciences & Emerging Technologies, Vol. 3, Issue . 2, pp.30-40, 2012

[19] I.A. Chidambaram, S. Velusami, "Design of decentralized biased controllers for load-frequency control of interconnected power systems", Electric Power Components and Systems, Vol.33, No.12, pp.1313-1331, 2005.

[20] K.Sabani, A. Sharifi, M. Aliyari sh, M.Teshnehlab, M. Aliasghary, "Load Frequency Control in Interconnected Power system using multi-objective PID controller", Journal of Applied Sciences Vol. 8, No.20, pp.3676-3682, 2008.

AUTHOR BIOGRAPHY

ND. Sridhar received Bachelor of Engineering in Electrical and Electronics Engineering (1996), Master of Engineering in Power System Engineering (2002) from Annamalai University, Annamalainagar, India. In 1997 he joined as lecturer in the in the Department of Electrical Engineering, Annamalai University and from 2010 he is working as Associate Professor in the Department of Electrical Engineering, Annamalai University, Annamalainagar, India. He is currently pursuing Ph.D degree in Electrical Engineering at Annamalai University, Annamalainagar. His research interests are in Power System Stability, Optimization Techniques, Distributed Generation, **sridarnd1@gmail.com**

I.A.Chidambaram received Bachelor of Engineering in Electrical and Electronics Engineering (1987), Master of Engineering in Power System Engineering (1992) and Ph.D in Electrical Engineering (2007) from Annamalai University, Annamalainagar. During 1988 - 1993 he was working as Lecturer in the Department of Electrical Engineering, Annamalai University and from 2007 he is working as Professor in the Department of Electrical Engineering, Annamalai University, Annamalainagar. He is a member of ISTE and ISCA. His research interests are in Power System stability and control, Restructured power system, Electrical Measurements and Control system. **driacdm@yahoo.com**

APPENDIX

A.1 Data for Thermal Reheat Power System [7]

Rating of each area = 2000 MW, Base power = 2000 MVA, f^o = 60 Hz, $R_1 = R_2 = R_3 = R_4$ = 2.4 Hz / p.u.MW, $T_{g1} = T_{g2} = T_{g3} = T_{g4}$ = 0.08 s, $T_{r1} = T_{r2} = T_{r1} = T_{r2}$ = 10 s, $T_{t1} = T_{t2} = T_{t3} = T_{t4}$ = 0.3 s, $K_{p1} = K_{p2}$ = 120Hz/p.u.MW, $T_{p1} = T_{p2}$ = 20 s, $\beta_1 = \beta_2$ = 0.425 p.u.MW / Hz, $K_{r1} = K_{r2} = K_{r3} = K_{r4}$ = 0.5, $2\pi T_{12}$ = 0.545 p.u.MW / Hz, a_{12} = -1.

A.2 Data for the HES unit [16]

K_{AE} = 0.002, T_{AE} = 0.5, K_{FC} = 0.01, TFC = 4

TABLE I. Optimized Controller parameters of the TATRIPS

TATRIPS	Controller gain of AREA 1		Controller gain of AREA 2	
	K_{p1}	K_{i1}	K_{p2}	K_{i2}
Case 1	0.341	0.459	0.191	0.081
Case 2	0.384	0.368	0.212	0.096
Case 3	0.428	0.396	0.236	0.127
Case 4	0.396	0.421	0.242	0.134
Case 5	0.412	0.436	0.253	0.139
Case 6	0.316	0.513	0.121	0.196
Case 7	0.336	0.527	0.139	0.184
Case 8	0.341	0.564	0.218	0.171
Case 9	0.357	0.568	0.247	0.195
Case 10	0.364	0.571	0.274	0.187
Case 11	0.384	0.576	0.277	0.175
Case 12	0.401	0.584	0.279	0.205
Case 13	0.419	0.587	0.286	0.237
Case 14	0.462	0.591	0.296	0.244

TATRIPS with HES unit	Controller gain of AREA 1		Controller gain of AREA 2	
	K_{p1}	K_{i1}	K_{p2}	K_{i2}
Case 1	0.228	0.484	0.102	0.091
Case 2	0.252	0.495	0.127	0.101
Case 3	0.287	0.521	0.134	0.122
Case 4	0.296	0.541	0.142	0.198
Case 5	0.328	0.532	0.154	0.201
Case 6	0.241	0.681	0.138	0.284
Case 7	0.283	0.698	0.148	0.302
Case 8	0.378	0.742	0.152	0.356
Case 9	0.398	0.771	0.165	0.347
Case 10	0.402	0.783	0.223	0.351
Case 11	0.427	0.813	0.286	0.374
Case 12	0.494	0.826	0.264	0.384
Case 13	0.538	0.795	0.271	0.412
Case 14	0.591	0.812	0.288	0.418

TABLE II. Optimized Controller parameters of the

TATRIPS with HES unit

TATRIPS	Setting time (τ_s) in sec			Peak over / under shoot		
	ΔF_1	ΔF_2	ΔP_{tie}	ΔF_1 in Hz	ΔF_2 in Hz	ΔP_{tie} in p.u.MW
Without HES units	18.14	17.52	20.13	0.321	0.215	0.082
With HES unit	3.394	3.254	5.649	0.117	0.042	0.017

TABLE III. Comparison of the system dynamic performance

for TATRIPS